



HAL
open science

Tuning the Charge Transfer in λ 5 -Phosphinines with Amino-substituents

Nicolas Ledos, Thitiporn Sangchai, Iryna Knysh, Manon H E Bousquet, Payal
Manzhi, Marie Cordier, Denis Tondelier, Bernard Geffroy, Denis Jacquemin,
Pierre-Antoine Bouit, et al.

► **To cite this version:**

Nicolas Ledos, Thitiporn Sangchai, Iryna Knysh, Manon H E Bousquet, Payal Manzhi, et al.. Tuning the Charge Transfer in λ 5 -Phosphinines with Amino-substituents. *Organic Letters*, 2022, 24 (37), pp.6869-6873. 10.1021/acs.orglett.2c02846 . hal-03773274

HAL Id: hal-03773274

<https://hal.science/hal-03773274>

Submitted on 9 Sep 2022

HAL is a multi-disciplinary open access archive for the deposit and dissemination of scientific research documents, whether they are published or not. The documents may come from teaching and research institutions in France or abroad, or from public or private research centers.

L'archive ouverte pluridisciplinaire **HAL**, est destinée au dépôt et à la diffusion de documents scientifiques de niveau recherche, publiés ou non, émanant des établissements d'enseignement et de recherche français ou étrangers, des laboratoires publics ou privés.

Tuning the Charge Transfer in λ^5 -Phosphinines with Amino-substituents

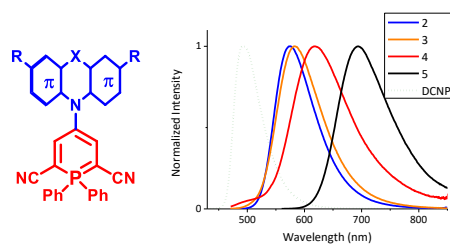
Nicolas Ledos,[†] Thitiporn Sangchai,[†] Iryna Knysh,[§] Manon H. E. Bousquet,[§] Payal Manzhi,^{‡,†} Marie Cordier,[†] Denis Tondelier,[‡] Bernard Geffroy,^{‡,†} Denis Jacquemin,^{§,*} Pierre-Antoine Bouit,^{†,*} Muriel Hisler^{†,*}

[†] Univ Rennes, CNRS, ISCR - UMR 6226, 35000 Rennes, France.

[§] CNRS, CEISAM UMR 6230, Nantes University, 44000 Nantes (France).

[‡] Laboratoire de Physique des Interfaces et des Couches Minces (LPICM), CNRS, Ecole Polytechnique, IP Paris, Palaiseau Cedex, France.

⁺ Université Paris-Saclay, CEA, CNRS, NIMBE, LICSEN, 91191, Gif-sur-Yvette, France



Tuning the charge transfer in λ^5 -phosphinines

ABSTRACT: We report the substitution of λ^5 -phosphinines (2,6-dicarbonitrile diphenyl-1- λ^5 -phosphinine) with amino-group. The impact of these modifications on both the optical and redox properties is investigated using a joint experimental/theoretical approach. In particular, we show that the choice of the donor diphenyl-amino group dramatically impacts the nature of the charge transfer. The use of di(methoxyphenyl)amine redshifts the optical properties and allows thermally activated delayed fluorescence in the solid-state. Finally, we demonstrated that λ^5 -phosphinines with amino-group can be used as active emitter in an electroluminescent device.

In the field of π -conjugated P-heterocycles based functional materials,¹ λ^5 -phosphinines recently emerged as promising fluorophores (Fig. 1). These compounds feature a phosphabenzene with an internal phosphorus ylide bond.² Their potential for luminescence applications was demonstrated in the seminal work of Müller *et al.*³ Later, it was also shown that π -extended λ^5 -phosphinines such **A** (Fig. 1) can be used as fluorescent emitters in Organic Light-Emitting Diodes (OLEDs).⁴ Hayashi *et al.* recently described an efficient synthesis of 2,6-dicarbonitrile diphenyl-1- λ^5 -Phosphinine (**DCNP**) based fluorophore **B** (Fig. 1).⁵ This organophosphorus scaffold is fully air and moisture stable and highly fluorescent. Adachi *et al.* further modified this building block to design efficient organic laser dyes and OLED without efficiency roll-off.⁶ However, no thermally activated delayed fluorescence (TADF) properties have been reported on these fluorophores to date.

TADF is a photophysical phenomenon characteristic of compounds featuring a small singlet-triplet energy gap and significant spin-orbit couplings (SOCs), allowing the triplet excitons to be up-converted to singlets through reverse intersystem crossing. Even if it is known for decades, it received a renewed attention recently since Adachi *et al.* showed that TADF

emitters such **4CzIPN** allows breaking the 5% theoretical limit of fluorescent OLEDs.⁷ Indeed, in TADF materials, both triplet and singlet excitons can generate light yielding to a potential Internal Quantum Efficiency (IQE) of 100%. The development of novel TADF emitters remains a blooming research area. One way to achieve TADF is to design Donor-Acceptor (D-A) systems in which the HOMO and LUMO are spatially separated, for example upon *ortho/meta* substitution on a phenyl ring, like in **4CzIPN**.⁸

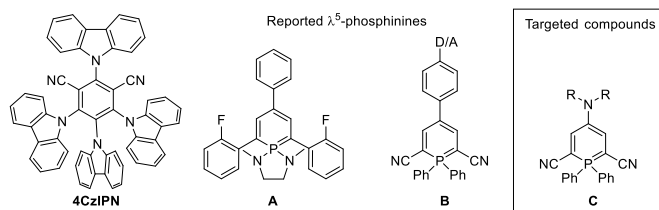
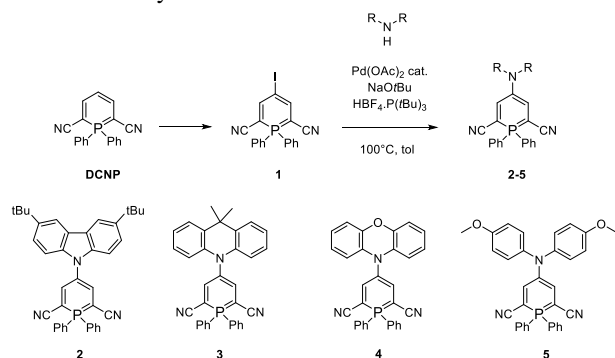


Figure 1: Chemical structure of **4CzIPN**, of reported λ^5 -phosphinines **A-B** and of targeted structures **C**.

To obtain the first TADF λ^5 -phosphinines, we decided to prepare D-A systems by connecting electron rich amines directly in *meta* position of the cyano groups in a structure reminiscent of **4CzIPN** (**C**, Fig. 1). In addition to the possibility of generating TADF, this structure affords an original platform to study the impact of charge transfer (CT) in λ^5 -phosphinines.

The fluorophore **2-5** were synthesized from the precursors **DCNP** and **1** for which the synthesis protocols described in the literature allow them to be obtained in good yields.^{5,9} The amines were then introduced on **1** using Buchwald-Hartwig coupling (Scheme 1). Fluorophores **2-5** were isolated in low to moderate yields. All the derivatives were fully characterized by multinuclear NMR, mass spectrometry, and X-ray diffraction for **3**.

Scheme 1: Synthesis of **2-5**



3 was characterized through X-ray (Fig. 2). **3** crystallizes in the P 2₁/c space group of the monoclinic system. The bond lengths within the λ^5 -phosphinine ring are classical and attest the conjugated ylidic nature of the P-C bond ($d = 1.75 \text{ \AA}$).⁵ The P-ring is globally planar (maximal deviation from the mean plane: 0.07 \AA) and the N-cycle lies almost perpendicularly to it (angle: 88°). Due to the bulkiness of the exocyclic P-Ph rings and the N-cycle, no clear intermolecular interactions are observed in the packing.

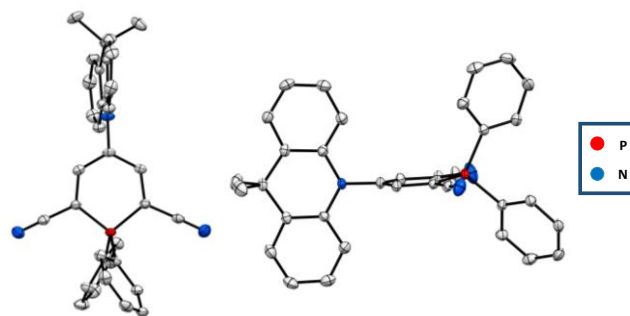


Figure 2: X-ray structure of **3**. Hydrogen atoms are omitted for clarity and thermal ellipsoids are set at 50% probability.

The electrochemical behavior of **2-5** was investigated by cyclic voltammetry in dichloromethane solution. All compounds display similar irreversible reduction wave characteristic of the DCNP ($E_{\text{red}} = -2.17 \text{ V vs Fc}^+/\text{Fc}$) (Table 1). In agreement with Balijapalli *et al*, all para-substituted DCNPs display two reversible oxidation waves (Fig. S2),¹⁰ the first corresponding to the oxidation of the electron rich amino group, the second to the oxidation of the λ^5 -phosphinine ring. The trend in the first oxidation potential nicely follows the increasing donor strength in the **2, 3, 4, 5** series (Table 1). The evolution of the second oxidation is not gradual with the increasing donor strength and is thus more difficult to rationalize.

The optical properties of **2-5** were investigated in diluted toluene solutions ($c = 10^{-5} \text{ mol.L}^{-1}$, Fig. 3 and Table 1). Despite the presence of electron-rich amino groups, **2-4** display similar visible absorption band as **DCNP** ($455 \text{ nm} < \lambda_{\text{abs}} < 465 \text{ nm}$, while $\lambda_{\text{DCNP}} = 458 \text{ nm}$, Table 1). This is somehow unexpected as π -extension with electron rich groups led to a redshift in the work of Hashimoto *et al* and Balijapalli *et al* (**B**, Fig 1).^{5,10} This outcome, rationalized by theory (see below), implies that the amino group is not involved in the transition responsible for the absorption, which is consistent with the neglectable solvatochromism in absorption (Fig. S3-6). This observation is also consistent with the X-ray structure of **3** showing a 90° angle between the DCNP fragment and the amino-cycle. In **4**, one notes nevertheless a shoulder at ca. 520 nm (Fig. 3), hinting at an extra weakly allowed absorption. In sharp contrast, **5** presents a redshifted absorption band with a lower extinction coefficient ($\lambda_{\text{abs}} = 529 \text{ nm}$, $\epsilon = 6000 \text{ L.Mol}^{-1}.\text{cm}^{-1}$) making it the most redshifted λ^5 -phosphinine described to date. In **5**, the redshifted absorption band suggests the presence of CT between the diphenylamine donor and the DCNP acceptor, which is corroborated by theoretical calculations (*vide infra*). All compounds also show luminescence in the visible with a redshift compared to **DCNP** ($\lambda_{\text{em}} = 491 \text{ nm}$). Indeed, a gradual bathochromic displacement is observed in the series **2-3-4-5**, in agreement with the increasing donor strength of the amine. This observation comes with a parallel decrease in luminescence quantum yields and the fluorescence lifetime, in agreement with the energy gap law (Table 1). In contrast to **2** which displays no clear solvatochromism in emission

(Fig. S3), **5** undergoes positive solvato-fluorochromism, a signature of CT (Fig S6). All compounds display luminescence lifetime in the order of the ns (either in aerated or degassed conditions), characteristic of pure fluorescence emission (and thus not of TADF, see Table 1 and S2). However, in the case of **5**, the approximated experimental Δ_{ST} (< 0.2 eV, Fig S7) confirms Adachi’s observation of DCNP having small singlet-triplet gap.^{6a} Theoretical calculations (in gas phase) confirms that only one triplet state of **5** is accessible ($\Delta_{ST} = 0.41$ eV) with a corresponding SOC of 0.27 cm^{-1} indicating possible, yet not optimal reverse intersystem crossing.

To get additional insights into the photophysical properties of the dyes, we have relied on first-principle calculations, and more precisely on the $cLR^2\text{-PCM-}\omega\text{B97X-D/6-311+G(2d,p)}$ approach (details in SI).¹¹ The main theoretical results are collected in Table 2. For absorption of DCNP, the lowest transition is strongly dipole-allowed and involves the central six-membered ring only (Fig. 4). The computed CT parameters indeed indicate a local transition (Table 2). In both **2** and **3**, for which the donor group is orthogonal to the core of the compound in the ground state, a similar picture emerges for absorption, consistent with the experimental observations (Figs. 3 and 4). In contrast in **4**, the lowest transition is almost dark and presents a pure CT character leading to a large electron-hole separation of 2.86 Å. The main absorption band at 455 nm experimentally in fact corresponds to the second excited state that presents a topology totally similar to the lowest one in DCNP, **2**, and **3**. The presence of this low-lying CT transition in **4** likely explains the tail at longer wavelength present in the experimental absorption (Fig. 3). Eventually, in **5**, the donating group is not perpendicular to the phosphinine core, and the two lowest transitions have significant CT characters, again consistent with the very different absorption spectrum measured for that compound. Interestingly, the lateral cyano substituents play a role in **4** and **5** while it is neglectable in DCNP, **2** and **3**. However, their presence is crucial to the overall chemical stability of all derivatives, in comparison with “classical” λ^5 -phosphinines.⁴

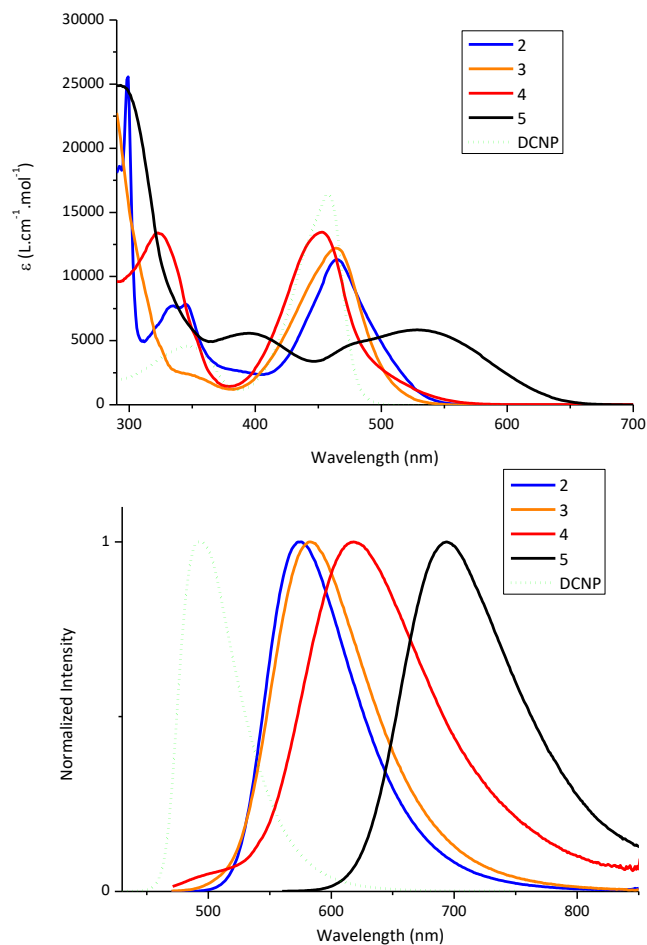


Figure 3: UV-vis absorption (up) and emission (down) of DCNP, **2-5** in diluted toluene solutions ($c = 10^{-5}\text{M}$)

Interestingly, Table 2 shows that while the vertical absorption wavelengths computed for DCNP and **2-4** are highly similar, their fluorescence counterparts strongly differ, which totally fits the experimental trend (Table 1 and Fig. 3), and indicates a strong geometrical relaxation of the excited state in **2-4**. Indeed, the orthogonality between the amine and the phosphinine moieties is lost in the excited state, which induces a significant local/CT mixed character for the emitting state, consistent with their stronger solvatochromism than for absorption (Fig. S3-5). For a more quantitative comparisons between theory and experiment, we report in Table 2 the TD-DFT 0-0 energies. On average, they are blueshifted by $+0.28$ eV as compared to the measured values, an error (at least partially) ascribable to the selected exchange-correlation functional (see CC2 values in Table S4). In the SI, we provide vibrationally-resolved fluorescence spectra obtained with TD-DFT, but they unsurprisingly show no peculiar shape (as their experimental counterpart Fig. 3), though the agreement with experiment is striking. More interesting are the computed radiative rates listed in Table 2. The theoretical values range from

5.4 (DCNP) to $0.9 \times 10^7 \text{ s}^{-1}$ (**4**), with the same order of magnitude and ranking as in the experiment, clearly confirming that the emissive state has been correctly identified by theory.

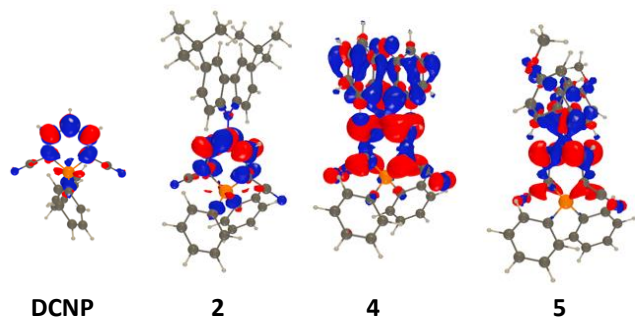


Figure 4: Density difference plots. Navy blue and crimson red lobes indicate decrease and increase of electron density upon absorption, respectively. Contour threshold: 2×10^{-3} au.

Due to its peculiar behaviour, additional photophysical characterization have been performed for **5** in solid state. While **5** does not fluoresce as pure powder or spin coated as pure material on glass substrate, it shows luminescence when blended in PMMA matrix (3% weight mass) ($\lambda_{em} = 680 \text{ nm}$, $\phi = 6\%$, Fig. S8). It should be noted that in the same conditions, **4** does not emit at all. More interestingly, in these conditions, at room temperature, **5** presents both prompt and delayed fluorescence components ($\tau_{PF} = 11.2 \text{ ns}$ and $\tau_{DF} = 1.44 \mu\text{s}$, Fig. S8). The delayed fluorescence is longer at low temperature ($\tau_{DF-298K}(\mathbf{5}) = 1.59 \mu\text{s}$) and the Φ_{DF}/Φ_{PF} ratio decreases from 298K to 77K : $\Phi_{DF}/\Phi_{PF}(298K) = 1.99$ et $\Phi_{DF}/\Phi_{PF}(77K) = 1.09$.¹² We checked that the emission at 77K occurs at similar wavelength than at rt (Fig. S8), thus ruling out the possibility of observing phosphorescence at low temperature. These observations indicate that **5** presents TADF in PMMA matrix. Even if this effect needs to be optimized, to our knowledge, **5** is thus the first TADF λ^5 -phosphinine.

Table 1: Measured optical and electrochemical data

	λ_{abs}^a (nm)	ϵ^a (L.Mol ⁻¹ .cm ⁻¹)	λ_{em}^a (nm)	$\phi^{a,b}$ (%)	λ_{0-0} (nm)	E_{0-0} (eV)	τ^a (ns, (%))	$k_r.10^{7a}$ (s ⁻¹)	$k_{nr}.10^{7a}$ (s ⁻¹)	E_{red}^c (V)	E_{ox1}^c (V)	E_{ox2}^c (V)
DCNP ^{6b,10}	458	16 000	491	97	473	2.62	10.4 (100)	8.8	-	-2.17	+0.82	x
2	465	11 000	575	62	521	2.38	18.9 (100)	3.3	2.0	-2.08	+0.50 ^d	+0.88 ^d
3	465	12 000	582	28	513	2.42	12.8 (100)	2.2	5.6	-2.06	+0.45 ^d	+0.70 ^d
4	455	13 000	618	2	535	2.32	4.9 (92); 14.2 (8)	0.4	17.5	-2.02	+0.31 ^d	+0.86 ^d
5	529	6 000	694	11	620	2.00	6.9 (88); 14.0 (12)	1.4	11.4	-2.10	+0.08 ^d	+0.46 ^d

^a In Toluene (10^{-5}M). ^b Measured in calibrated integration sphere. ^c($c = 10^{-3} \text{ M}$) recorded in CH_2Cl_2 with $\text{Bu}_4\text{N}^+\text{PF}_6^-$ (0.2 M) at a scan rate of 200 mVs^{-1} . Potentials vs Fc^+/Fc . ^d quasi-reversible process

Table 2: Main TD-DFT results computed in toluene: vertical absorption wavelength and corresponding oscillator strength, CT parameters for absorption, fluorescence wavelengths, 0-0 energies and radiative rate constant (see the SI for details).

	Transition	$\lambda_{vert-abs}$ (nm)	f	D^{CT} (Å)	q^{CT} (e)	$\lambda_{vert-fluo}$ (nm)	E_{0-0} (eV)	k_r (10^7 s^{-1})
DCNP	S_0-S_1	386	0.238	0.10	0.44	429	3.00	5.4
2	S_0-S_1	386	0.201	0.21	0.46	499	2.68	2.8
3	S_0-S_1	395	0.196	0.03	0.45	509	2.69	1.9
4	S_0-S_1	446	0.000	2.86	1.22	551	2.51	0.9
	S_0-S_2	387	0.201	0.02	0.45	na	na	
5	S_0-S_1	484	0.109	2.46	0.77	606	2.24	1.4
	S_0-S_2	348	0.070	2.07	0.64	na	na	

Given its satisfying thermal properties ($Td_{10} = 353^\circ\text{C}$, Fig. S12) associated with suitable redox properties and presence of TADF emission in solid matrix, the electroluminescent properties of **5** were evaluated in a multi-layered OLED device (details in SI). The use of various doping rates of **5** in either CBP (4,4'-Bis(N-carbazolyl)-1,1'-biphenyl) or mCP (1,3-Bis(N-carbazolyl)benzene) matrices only led to low external quantum efficiency (EQE) and brightness ($\text{EQE} < 0.4\%$, $\text{B} < 86 \text{ cd.m}^{-2}$, Table S3). Such low emission originates from various factors. First, the luminescence quantum yields of **5** in the matrix are low, e.g., it attains 10% only for **5** diluted in CBP (12% weight). In addition, in these conditions, no delayed fluorescence was detected (Fig. S13). These results illustrate that the intermolecular interactions with the matrix are key parameters to obtain TADF with this λ^5 -phosphinine. Such phenomenon has already been observed with several other fluorophores, but remain poorly

understood in term of structure properties relationships.¹³ However, these results remain promising as the OLED is very stable and presents a brightness increasing until very high current densities (300 mA.cm^{-2}).

In this letter we report the substitution of 2,6-dicarbonitrile diphenyl-1- λ^5 -Phosphinine with diphenyl-amino donor group in *meta* to the cyano substituents groups in a structure reminiscent of **4CzIPN**. Four new fluorophores were prepared and fully characterized. Using a joint experimental and theoretical approach, we show that the optical properties depend on a complex interplay between the amino-donor group and the λ^5 -phosphinine acceptor. In particular, with di(methoxyphenyl)amine we could redshift the optical properties of compound **5** and observe TADF in PMMA matrix. Finally, the redox and thermal properties of **5** allowed to prepare stable OLED device, thus

paving the way toward molecular engineering of λ^5 -phosphinines toward efficient TADF OLED devices.

ASSOCIATED CONTENT

Supporting Information

Synthetic procedure, complete characterizations, X-ray crystallographic data and CIF files, computational details and Cartesian coordinates. The Supporting Information is available free of charge on the ACS Publications website.

AUTHOR INFORMATION

Corresponding Author

*E-mail : Denis.Jacquemin@univ-nantes.fr

*E-mail: pierre-antoine.bouit@univ-rennes1.fr

*E-mail: muriel.hissler@univ-rennes1.fr

Author Contributions

The manuscript was written through contributions of all authors. / All authors have given approval to the final version of the manuscript.

ACKNOWLEDGMENT

This work is supported by the *Ministère de la Recherche et de l'Enseignement Supérieur*, the CNRS, the *Région Bretagne* (ARED grant to NL), the French National Research Agency (ANR Fluohyb ANR-17-CE09-0020 and BSE-forces ANR-20-CE29-005). Y. Molard and G. Taupier (Scanmat-UMS 2001) are thanked for PLQY measurements. IK, MHEB, and DJ are indebted to the CCIPL computational center for the very generous allocation of computational time.

REFERENCES

- (1) (a) Duffy, M. P.; Delaunay, W.; Bouit, P.-A.; Hissler, M. Conjugated phospholes and their incorporation into devices: components with a great deal of potential *Chem. Soc. Rev.* **2016**, *45*, 5296–5310; (b) Ren, Y.; T. Baumgartner, Combining form with function – the dawn of phosphole-based functional materials. *Dalton Trans.* **2012**, *41*, 7792–7800.; (c) Grzybowski, M.; Taki, M.; Senda, K.; Sato, Y.; Ariyoshi, T.; Okada, Y.; Kawakami, R.; Imamura, T.; Yamaguchi, S. A Highly Photostable Near-Infrared Labeling Agent Based on a Phospho-rhodamine for Long-Term and Deep Imaging *Angew. Chem. Int. Ed.* **2018**, *57*, 10137–10141.
- (2) a) Märkl, G.; 1,1-Diphenyl-1-phosphabenzene, *Angew. Chem. Int. Ed.* **1963**, *2*, 479; b) Dimroth, K. (1973). Delocalized phosphorus-carbon double bonds. In: Phosphorus-Carbon Double Bonds. Fortschritte der Chemischen Forschung, vol 38/1. Springer, Berlin, Heidelberg. c) Huang, J.; Tarábek, J.; Kulkarni, R.; Wang, C.; Dračinský, M.; Smales, G. J.; Tian, Y.; Ren, S.; Pauw, B. R.; Resch-Genger, U.; Bojdys, M. J. A pi-Conjugated, Covalent Phosphinine Framework *Chem. Eur. J.* **2019**, *25*, 12342-12348.
- (3) Müller, C.; Wasserberg, D.; Weemers, J. J. M.; Pidko, E. A.; Hoffmann, S.; Lutz, M.; Spek, A. L.; Meskers, S. C. J.; Janssen, R. A. J.; van Santen R. A.; Vogt, D. Donor-Functionalized Polydentate Pyrylium Salts and Phosphinines: Synthesis, Structural Characterization, and Photophysical Properties, *Chem. Eur. J.* **2007**, *13*, 4548-4559.
- (4) Pfeifer, G.; Chahdoura, F.; Papke, M.; Weber, M.; Sziucs, R.; Geffroy, B.; Tondelier, D.; Nyulász, L.; Hissler, M.; Müller, C. Synthesis, Electronic Properties and OLED Devices of Chromophores Based on λ^5 -Phosphinines, *Chem. Eur. J.* **2020**, *26*, 10534-10543.
- (5) Hashimoto, N.; Umamo, R.; Ochi, Y.; Shimahara, K.; Nakamura, J.; Mori, S.; Ohta, H.; Watanabe, Y.; Hayashi, M., Synthesis and Photo-physical Properties of λ^5 -Phosphinines as a Tunable Fluorophore. *J. Am. Chem. Soc.* **2018**, *140* (6), 2046-2049
- (6) a) Karunathilaka, B. S. B.; Balijapalli, U.; Senevirathne, C. A. M.; Esaki, Y.; Goushi, K.; Matsushima, T.; Sandanayaka, A. S. D.; Adachi, C.; An Organic Laser Dye having a Small Singlet-Triplet Energy Gap Makes the Selection of a Host Material Easier *Adv. Funct. Mater.* **2020**, *30*, 2001078; b) Tang, X.; Balijapalli, U.; Okada, D.; Karunathilaka, B. S. B.; Senevirathne, C. A. M.; Lee, Y.; Feng, Z.; Sandanayaka, A. S. D.; Matsushima, T.; Adachi, C.; Electron-Affinity Substituent in 2,6-Dicarbonitrile Diphenyl- λ^5 -Phosphinine Towards High-Quality Organic Lasing and Electroluminescence under High Current Injection, *Adv. Funct. Mater.* **2021**, *31*, 2104529.
- (7) a) Endo, A.; Sato, K.; Yoshimura, K.; Kai, T.; Kawada, A.; Miyazaki, H.; Adachi, C. Efficient up-conversion of triplet excitons into a singlet state and its application for organic light emitting diodes, *Appl. Phys. Lett.* **2011**, *98*, 083302; b) Uoyama, H.; Goushi, K.; Shizu, K.; Nomura, H., Adachi, C. Highly efficient organic light-emitting diodes from delayed fluorescence, *Nature* **2012**, *492*, 234-238; c) Hong, G.; Gan, X.; Leonhardt, C.; Zhang, Z.; Seibert, J.; Busch, J. M.; Bräse, S. A Brief History of OLEDs-Emitter Development and Industry Milestones, *Adv. Mater.* **2021**, *33*, 2005630
- (8) a) Im, Y.; Kim, M.; Cho, Y. J.; Seo, J.-A.; Yook, K. S.; Lee, J. Y. Molecular Design Strategy of Organic Thermally Activated Delayed Fluorescence Emitters *Chem. Mater.* **2017**, *29*, 1946–1963; b) Liang, X.; Tu, Z. L.; Zheng, Y.-X.; Thermally Activated Delayed Fluorescence Materials: Towards Realization of High Efficiency through Strategic Small Molecular Design, *Chem. Eur. J.* **2019**, *25*, 5623-5642.
- (9) Yoshimura, A.; Kimura, H.; Handa, A.; Hashimoto, N.; Yano, M.; Mori, S.; Shirahata, T.; Hayashi, M.; Misaki, Y. Synthesis, structures, and electrochemical and optical properties of λ^5 -phosphinine derivatives functionalized tetrathiafulvalene analogs, *Tetrahedron Letters* **2020**, *61*, 151724.
- (10) Balijapalli, U.; Tang, X.; Okada, D.; Lee, Y.; Karunathilaka, B. S. B.; Auffray, M.; Tumen-Ulzii, G.; Tsuchiya, Y.; Sandanayaka, A. S. D.; Matsushima, T.; Nakanotani, H.; Adachi, C. 2,6-Dicarbonitrile Diphenyl- λ^5 -Phosphinine (DCNP)-A Robust Conjugated Building Block for Multi-Functional Dyes Exhibiting Tunable Amplified Spontaneous Emission *Adv. Optical Mater.* **2021**, *9*, 2101122
- (11) cLR²: a) Guido, C. A.; Chrayteh, A.; Scalmani, G.; Mennucci B.; Jacquemin, D.; Simple Protocol for Capturing Both Linear-Response and State-Specific Effects in Excited-State Calculations with Continuum Solvation Models, *Chem. Theory Comput.* **2021**, *17*, 5155-5164; ω b97X-D: b) Chai, J.-D.; Head-Gordon, M. Long-range corrected hybrid density functionals with damped atom-atom dispersion corrections, *Phys. Chem. Chem. Phys.* **2008**, *10*, 6615-6620.
- (12) Φ_{PF}/Φ_{DF} ratio determination: Nakagawa, T.; Ku, S.-Y.; Wong, K.-T.; Adachi, C.; Electroluminescence based on thermally activated delayed fluorescence generated by a spirobifluorene donor-acceptor structure, *Chem. Commun.* **2012**, *48*, 9580-9582.
- (13) (a) Méhes, G.; Goushi, K.; Potsavage Jr, W. J.; Adachi, C.; Influence of host matrix on thermally-activated delayed fluorescence: Effects on emission lifetime, photoluminescence quantum yield, and device performance, *Org. Elec.* **2014**, *15*, 2027-2037. (b) Li, N.; Ni, F.; Huang, Z.; Cao, X.; Yang, C. Host-Dopant Interaction between Organic Thermally Activated Delayed Fluorescence Emitter and Host Material: Insight into the Excited State, *Adv. Opt. Mater.* **2022**, *10*, 2101343.